Deep-Sea Research, Vol. 37, No. 8, pp. 1197–1211, 1990.
Printed in Great Britain.

0198-0149/90 $3.00 + 0.00

RAPID RESPONSE PAPER

A model of the formation of marine algal flocs by physical coagulation processes

GEORGE A. JACKSON*

(*Received* 16 *January* 1990; *in revised form* 29 *April* 1990; *accepted* 9 *May* 1990)

Abstract—Aggregates of organic matter ("marine snow") are highly visible phenomena in oceanic waters which can control material fluxes to the deep sea. These aggregates take many forms and undoubtedly have many causes. One form frequently described is that composed of algae, usually diatoms, occurring after an algal bloom. A model combining kinetic coagulation theory and simple algal growth kinetics describes the dynamics of such an algal bloom. Results show this to be a two-state system in which coagulation processes are either unimportant when algal concentrations are low or dominant when they are high, with a rapid transition between the two states. Critical algal concentration for this transition is inversely related to fluid shear, algal size and stickiness, and is similar to values observed after a bloom. The role of coagulation in controlling particle dynamics for more complicated aquatic systems will depend on other biological particle production and consumption processes, such as zooplankton feeding and defecation. These results emphasize the importance of measuring algal sizes and abundances when studying floc formation.

INTRODUCTION

AGGREGATES are frequently observed in the ocean after algal blooms. The role that physical aggregation processes may have in their formation has been noted, as has the importance of resulting flocs falling to the benthos (BILLET *et al.*, 1983; SMETACEK, 1985; SMETACEK and POLLEHNE, 1986; ALLDREDGE and GOTSCHALK, 1988a,b; ALLDREDGE and SILVER, 1988, KRANCK and MILLIGAN, 1988). There has been laboratory production of such flocs using mixtures of organic materials (KRANCK and MILLIGAN, 1980) and naturally occurring organic matter (SHANKS and EDMONDSON, 1989). Despite the awareness of coagulation processes, coagulation theory has not been applied to analyse these marine algal blooms.

Previous applications of coagulation theory to marine systems have emphasized aggregation of inorganic particles. The observed particle size spectra are consistent with those which would result from coagulation processes (HUNT, 1982). Shear coagulation has been observed to be important in the high particle concentration, high shear environment of the benthic boundary layer but likely to be less important in the more tranquil mid-water regime (MCCAVE, 1984).

*Department of Oceanography, Texas A&M University, College Station, TX 77843, U.S.A.

Kinetic coagulation theories which have been applied to explain the nutrient and particle dynamics in lakes assume nutrient limitation of algal growth rate or constant algal production rates (O'MELIA, 1972; O'MELIA and BOWMAN, 1984; WEILENMANN *et al.*, 1989). An important conclusion of these studies has been that rates of algal losses to coagulation can be comparable to losses caused by zooplankton grazing (WEILENMANN *et al.*, 1989).

In this paper, a model is developed of an algal bloom which includes coagulation in conjunction with algal growth. Results include a simple equation showing conditions when coagulation is important for controlling algal concentrations and settling.

MODEL

An aggregate is a particle formed by collision of two smaller particles; large aggregates are formed by the repetitive collision and coalescence of smaller ones (O'MELIA, 1972; PRUPPACHER and KLETT, 1980; MCCAVE, 1984). Non-aggregate particles are formed by a variety of mechanisms, of which algal division is the one used here. A particle is lost when it is incorporated into a larger particle after a collision or when it sinks out of the system. Coagulation theory describes the rate of change in concentrations of a size class by adding the rates of all particle collisions which form aggregates of the size class, subtracting the rates of all collisions involving particles of the size which form larger particles, and subtracting the rate of particle loss to settling. Particle dynamics are determined by all these processes working simultaneously on particles of all size classes.

Collision rate is a function of sizes of colliding particles, their concentrations, and environmental parameters. Three mechanisms are used to describe particle collisions in aquatic systems. The first is Brownian motion, in which the random motions of particles move some together. Because the diffusivity of particles varies inversely with their radii, small particles move the most and have the greatest collision rates (Fig. 1). The second collision mechanism is shear, either laminar or turbulent, in which differences in fluid velocity cause two particles being carried by the fluid to approach each other and touch. The third collision mechanism is differential sedimentation, in which one particle falls faster than another, overtaking and colliding with it. Because particle fall velocity is usually a function of size, two particles of the same size and specific gravity fall at the same rate and do not overtake each other.

All particles can be described in terms of the number of single algal cells i that they contain. The collision rate of two particles of sizes i and j is given by $C_iC_j\beta_{ij}$, where C_i and C_j denote the concentrations (abundances) of particles containing i and j algal units and where the coagulation kernal β_{ij} is the sum of terms describing the different processes that bring particles into contact: Brownian motion (β_{Bij}), differential sedimentation (β_{Dij}) and shear (β_{Sij}) (Fig. 1).

In this formulation, the ultimate source of all particulate matter is the division of algae, usually solitary, at a specific growth rate μ. Division of solitary algae leads to additional solitary algae, not aggregates with two algal cells. The ultimate sink is the settling out of a layer. The effect of sinking on particle concentration is given by the flux (w_iC_i) divided by the mixed layer depth, z, where w_i is the particles settling rate. If α is the probability that particles stick after contact (stickiness), r_i is particle radius, and the Kronecker delta δ_{ij} is used to account for the loss of two particles when both colliding particles are of the same size, then

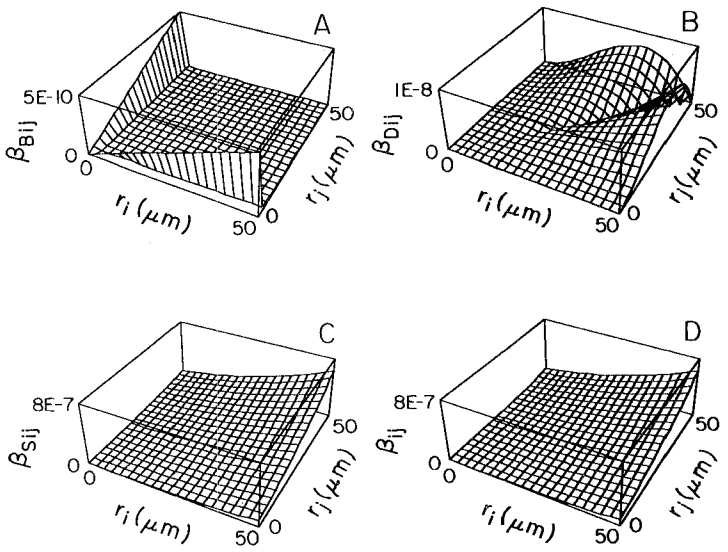

Fig. 1. The collision kernal (β_{ij}) as a function of r_1, r_2 for Brownian motion, $\beta_{Bij} = 4\pi(D_i + D_j)(r_i + r_j)$ (A), differential sedimentation, $\beta_{Dij} = 0.5\pi r_i^2(w_i - w_j)$, $i < j$ (B), shear, $\beta_{Sij} = 1.3\gamma(r_i + r_j)^3$ (C), and the total, $\beta_{ij} = \beta_{Bij} + \beta_{Dij} + \beta_{Sij}$ (D). D_i is the diffusivity of a particle, $D_i = kT(6\pi\eta r_i)^{-1}$, where T is the absolute temperature, k is the Boltzman constant, and η is the viscosity (PRUPPACHER and KLETT, 1980). X and Y axes are the sizes of the two interacting particles. The Z axis gives the magnitude of the interactions in units of $cm^3\ s^{-1}$ part.$^{-1}$. The shear $\gamma = 2\ s^{-1}$.

$$\frac{dC_1}{dt} = \mu C_1 - \alpha C_1 \sum_{i=1}^{\infty} C_i\beta_{1i}(1 + \delta_{1i}) - C_1 w_1 z^{-1} \tag{1}$$

$$\frac{dC_i}{dt} = 0.5\alpha \sum_{j=1}^{i-1} C_j C_{i-j}\beta_{j,i-j} - \alpha C_i \sum_{j=1}^{\infty} (1 + \delta_{ij})C_j\beta_{ij} - C_i w_i z^{-1} \quad \text{for } i \neq 1. \tag{2}$$

Because the effect of Brownian motion is small for particles larger than about 1 μm (MCCAVE, 1984), β_{Bij} is not included in these calculations.

The model can be modified to include the case where cells in aggregates divide at the same specific growth rate as the solitary cells. Such growth increases the aggregate's size, moving it into a larger size class. If single cells divide to form two single cells but all other particles keep their daughter cells when there is a cell division, then equation (2) must be modified by adding the terms $-2\mu C_2$ for $i = 2$ and $+\mu[(i-1)C_{i-1} - iC_i]$ for $i > 2$.

The model can be expanded to describe a situation with several layers, each internally well mixed. For the case of sub-surface layers, $l > 1$, the inclusion of terms for particles entering from above results in

$$\frac{dC_{1,l}}{dt} = \mu C_{1,l} - \alpha C_{1,l} \sum_{i=1}^{\infty} C_{i,l}\beta_{1i,l}(1 + \delta_{1i}) + (C_{1,l-1} - C_{1,l})w_1 z_l^{-1} \tag{3}$$

$$\frac{dC_{i,l}}{dt} = 0.5\alpha \sum_{j=1}^{i-1} C_{j,l}C_{i-j,l}\beta_{j,i-j,l} - \alpha C_{i,l}\sum_{j=1}^{\infty}(1+\delta_{ij})C_{j,l}\beta_{ij,l}$$

$$+ (C_{i,l-1} - C_{i,l})w_i z_l^{-1} \quad \text{for } i \neq 1, \tag{4}$$

where the additional subscript l denotes the layer-specific variables. The equations for the top layer stay the same.

To calculate r_i and w_i, relationships typical for phytoplankton were used: $\phi_i = i\phi_1 = br_i^{2.28}$, where ϕ_i is the carbon content (nmol) of an aggregate of i units (Mullin *et al.*, 1966), $b = 1.67 \times 10^5$ nmol cm$^{-2.28}$ particle^{-1}; $w_i = 2\xi r_i^{1.17}$, where $\xi = 1.24$ cm$^{-0.17}$ s^{-1} (SMAYDA, 1970; JACKSON, 1989). The relationship between r_i and i simplifies to $r_1 i^{0.44}$. These describe aggregate as well as algal properties: a 1 mm diameter aggregate is about 10 μg dry wt and sinks at about 0.035 cm s^{-1} (ALLDREDGE and GOTSCHALK, 1988b); these relationships predict a mass of 2.2 μg C (equivalent to 5.5 μg dry wt for a dry wt to C ratio of 2.5 (PARSONS *et al.*, 1961) and a sinking rate of 0.037 cm s^{-1}.

These equations were solved numerically using the DEABM subroutine in the SLATEC package for a system with a maximum i, i_{max}, of either 400 or 1600 for several values of γ, α and μ. The initial concentration values were $C_1 = 0.1$ part. cm^{-3}, while those of the aggregates were given by $C_1(ii_{max})^{-1}$.

Model results are concentrations for each size category, effectively $C_i = dC/di$, particle size spectrum in terms of i. This can be converted to a conventional spectrum in terms of particle radius by noting that

$$\frac{dC}{dr} = \frac{dC}{di}\frac{di}{dr}$$

$$= (0.44r_1)^{-1} i^{0.56}\frac{dC}{di}. \tag{5}$$

Particle size distributions are frequently presented in terms of the accumulated particle concentration,

$$N(a) = \int_a^{\infty} \frac{dC}{da}\,da$$

$$N(r_i) = \sum_{j=i}^{i_{max}} C_j. \tag{6}$$

Simulations were run for a range of initial conditions. The results were similar to those shown for $\gamma = 2$ s^{-1}, $\mu = $ d^{-1}, $\alpha = 0.25$, and $i_{max} = 1600$ (Fig. 2).

RESULTS

Coagulation has little effect on the single algal cells early in a bloom, because of the low phytoplankton concentrations and the square dependence of coagulation rates on particle concentration (Fig. 2). Single algal concentrations increase exponentially with time as the cells divide while aggregate concentrations decrease as they slowly settle out. Coagulation

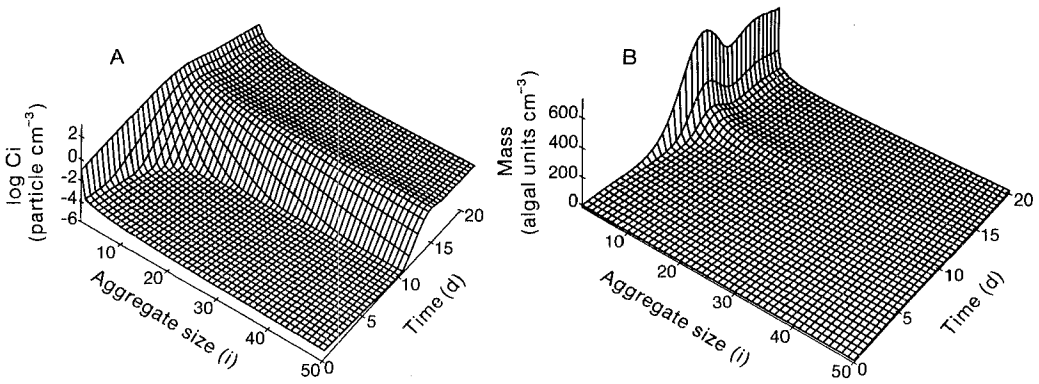

Fig. 2. Population growth for algae dividing exponentially and forming aggregates. X and Y axes are time and aggregate size; Z axes are log(concentration) (A) and linear biomass (B). The aggregate size ranges from 1 (the solitary alga) on the left to 50 algal components on the right. The time ranges from day 0 at the front to day 20 at the back. Exponential increase of C_1 is halted when algal abundance reaches a critical concentration despite its continued cell divisions. All new cells are channeled into larger aggregates and, ultimately, escape the sytstem by settling out. Parameter values are: $r_1 = 10\,\mu$m, $z = 20$ m, $\mu = 1\ \mathrm{d}^{-1}$, $\gamma = 2\ \mathrm{s}^{-1}$ and $\alpha = 0.25$.

becomes important over a short period of time, resulting in rapid increase in concentrations of larger particles. This change occurs at about day 11 here, when C_1 reaches its maximum, 708 cell cm^{-3}. Over the course of a day, single cell concentrations stop increasing and even decrease slightly to 550 cell cm^{-3} by day 16, when the particle size distribution achieves a steady-state spectrum. The change occurs most rapidly for the largest particles: C_{400} changes from 8.5×10^{-6} to 1.4×10^{-4} and C_{1600} from 7.8×10^{-10} to 1.5×10^{-6} part. cm^{-3} in half a day. There is no further increase after this transition and even a slight decrease in particle concentrations despite the continued division of the single algae. All new particle production is fed into production of aggregates, which ultimately settle out of the system. Were the algae to stop growing, the continued coagulation and sinking would cause particle concentrations to decrease. Coagulation makes the algal bloom a system with two states: one the simple exponential increase in solitary cells, the other limitation of algal concentration and control of algal settling by coagulation.

Simulating the system with fewer size classes, $i_{\max} = 400$ rather than $i_{\max} = 1600$, decreases the number of interactions considered. For the coagulation loss of single cells to balance cell growth, concentrations must be higher (Fig. 3). Differences between the two are relatively small, being highest for large aggregates: values of C_{400} are 1.2×10^{-3} and 6.9×10^{-4} part. cm^{-3} s^{-1} for $i_{\max} = 400$ and 1600, respectively.

The ultimate sink of all the material produced by the dividing algae should be loss by aggregate sinking. The differences are greater between the $i_{\max} = 400$ and 1600 cases (Fig. 4). The total amounts of material falling out of the system are 6.1 and 8.0 algal units cm^{-2} s^{-1} for $i_{\max} = 400$ and 1600, respectively. These are 48 and 63% of the total integrated particle production of 12.7 algal units cm^{-2} s^{-1}. The use of smaller $i_{\max}$ causes a greater discrepancy predicting fluxes than concentrations because of the greater importance of settling by the larger particles that are more poorly predicted. Breakup of aggregates by higher shear limits the size that aggregates can take (e.g. McCave, 1984).

The pattern for particle increase is modified when algae on the flocs can also grow (Fig.

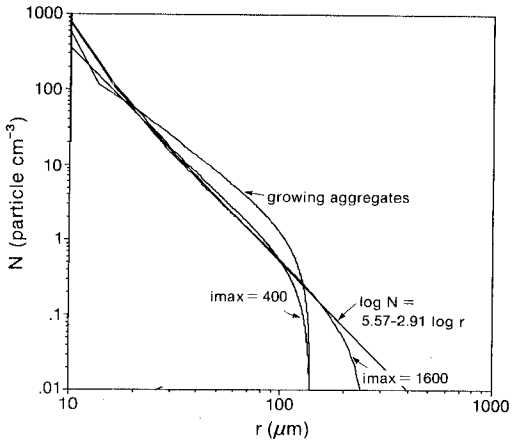

Fig. 3. Cumulative number of particles, N, as function of particle radius for standard cases with $i_{max} = 400$ and 1600, and for the case of algae growing in aggregates with $i_{max} = 400$. Linear fits to the log-transformed data give curve fits of $\log N = 5.39 - 2.84 \log r(\mu m)$ for the standard $i_{max} = 1600$, $\log N = 5.57 - 2.91 \log r(\mu m)$ for the standard, $i_{max} = 400$, $\log N = 4.97 - 2.41 \log r(\mu m)$ for the growing aggregate cases. Fits were calculated using points with $r \leq 100\,\mu m$ when $i_{max} = 400$ and $r \leq 160\,\mu m$ when $i_{max} = 1600$. The line resulting for the first case is shown.

5). Aggregate concentrations decrease during the early growth phase as cellular division in aggregates forms larger aggregates which sink rapidly and which are not replenished by the formation of new aggregates. With the formation of dimers ($i = 2$ particles), aggregates begin to form. Coagulation still dominates at high concentrations, placing a maximum on the algal concentrations. Maximum C_1 is lower, 562 as opposed to the earlier 708 part. cm^{-3} s^{-1}, because of the higher concentrations of other particles. Coagulation places a maximum on single cell concentrations that is still within a factor of two of that when only single cells divide.

The limits on single cell algal concentrations can be estimated by noting that the first,

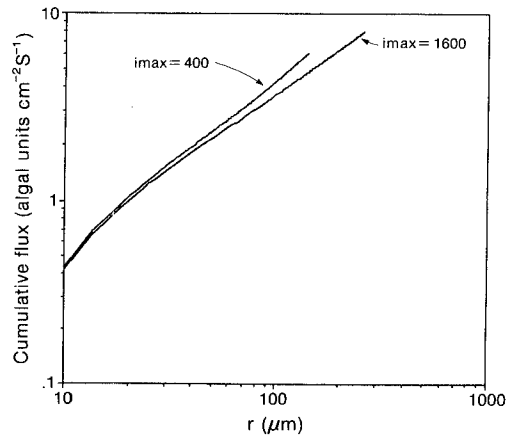

Fig. 4. Cumulative settling fluxes as functions of particle radius for the standard $i_{max} = 400$ and 1600 cases. Accumulation here is from small to large, the reverse of that used for calculations of N.

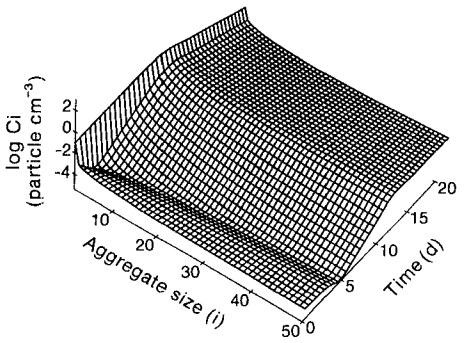

Fig. 5. Population growth for the case of algae dividing exponentially while in the aggregates forming aggregates. X and Y axes are time and aggregate size, respectively; Z axis is log(concentration). Parameter values as in Fig 2.

crucial step is the production of the dimer. Even after equilibrium has been achieved, the dominant loss of single algal cells is collision with other single cells (Fig. 6). Simplifying equation (1) yields

$$\frac{dC_1}{dt} = \hat{\mu}C_1 - \alpha\beta_{11}C_1^2, \tag{7}$$

where $\hat{\mu} = \mu - w_1 z^{-1}$ is the modified specific growth rate, the rate at which the algal population would grow if there were no coagulation. $\beta_{D11} = 0$ is zero because two equal-sized particles fall at the same rate and cannot overtake each other to collide. As a result, β_{11} reduces to $\beta_{S11} = 10.4\gamma r_1^3$ (Fig. 1). The population stops growing when $dC/dt = 0$, implying that the maximum concentration (C_{cr}) is given by $C_{cr} = 0.048\hat{\mu}(\alpha\gamma)^{-1} r_1^{-3}$. These abundances can be calculated as particulate nitrogen concentrations (N_{cr}) by

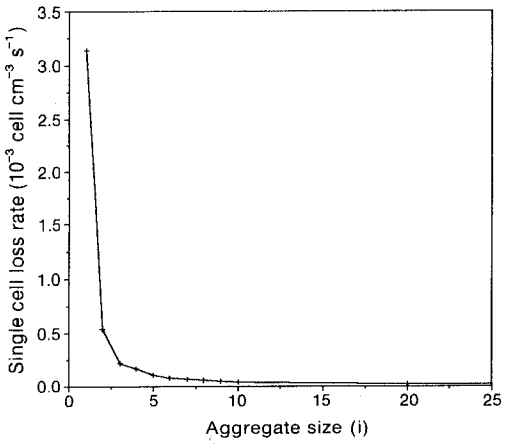

Fig. 6. Rate of loss of single algal cells from collision = $\alpha C_1 C_i \beta_{1i}(1 + \delta_{1i})$. The total losses, including the small loss to settling, equal the gains from cellular division when the size distribution is steady state. For this example, $\mu C_1 = 6.36 \times 10^3$ cell cm^{-3} s^{-1}.

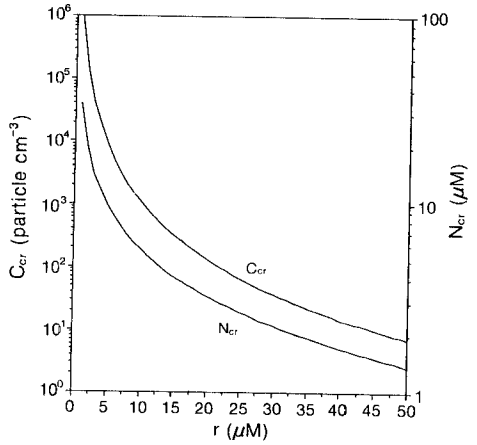

Fig. 7. Critical particle concentrations (upper line) and particulate nitrogen (lower line) concentrations as a function of algal radius: $\mu = 1\ \mathrm{d}^{-1}$, $\gamma\alpha = 0.5\ \mathrm{s}^{-1}$.

assuming a C:N value of 6 (PARSONS *et al.*, 1961) and using the above expression for algal C content, $N_{cr} = 0.008\, b(\mu - w_1 z^{-1})(\alpha\gamma)^{-1} r_1^{-0.76}$.

The strong size dependence of C_{cr} and N_{cr} can be seen for $\alpha\gamma = 0.5\ \mathrm{s}^{-1}$ (Fig. 7). C_{cr} and N_{cr} are 8.9×10^6 cell cm^{-3} and 58 μM for $r_1 = 0.5\,\mu$m and as few as 6.9 cell m^{-3} and 1.36 μM for $r_1 = 50\,\mu$m. Coagulation is a more important constraint for larger cells, such as some of the diatoms, than it is for small cyanobacteria.

If the 20 m mixed layer in the original simulation is divided into four layers of 5 m thickness each, particle concentrations, especially of the larger particles, increase with depth (Fig. 8). In this case, $\gamma = 1\ \mathrm{s}^{-1}$, half that of the previous case, resulting in $C_{1,l}$ concentrations which are twice as high as those in Fig. 2 but nearly identical between

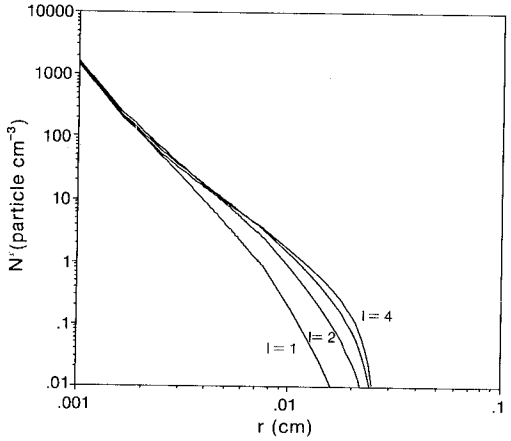

Fig. 8. Steady-state particle size spectra for four different layers when other parameters are the same for all layers: $z_l = 5$ m, $\gamma = 1\ \mathrm{s}^{-1}$, $\alpha = 0.25$, and $i_{\max} = 1600$. $C_{1,1}$ and $C_{1,4}$ (concentrations of single cells in top and bottom layers) equal 1150 and 1050 cell cm^{-3}. Slopes of lines fit through the log-transformed N as fn of r data for $r \leq 0.01$ cm were -3.64, -3.00, -2.71 and -2.61 for layers 1, 2, 3 and 4, respectively.

layers: $C_{1,1}$ = 1150 and $C_{1,4}$ = 1050 cells cm^{-3}. Largest particles show the largest concentration differences between top and bottom, with $C_{1600,4}/C_{1600,1}$ = 208.

Layers with decreasing shear show some of the expected patterns. Consider the shear to be inversely proportional to depth, as might be observed for wind-driven turbulence. Estimating the shear as that of the midpoint of each 5 m layer, then for a shear of 1 s^{-1} at 1 m depth, the shear will range from 0.4 s^{-1} in the top layer to 0.057 s^{-1} in the fourth layer. The values of $C_{1,1}$ and $C_{1,4}$ are 2880 and 17,400 cell cm^{-3}, which are 52 and 45% of their respective C_{cr} (Fig. 9). Being in the lower layer again increases the concentrations of the larger particles, with $C_{1600,4}/C_{1600,1}$ = 550. Despite the higher C_{cr} for the lower layer, which would require 1.8 days more to reach at the μ = 1, the transition to the coagulation-controlled region is in fact sooner by 2–3 days (Fig. 10).

DISCUSSION

This implementation of a coagulation model has as its basic unit the algal cell rather than the more often used particle radius or volume (e.g. O'Melia, 1972; Hunt, 1982; McCave, 1984). The algal cell approach has several advantages as well as some disadvantages. Advantages are that it is easy to track particle mass, which is $i\phi_i$, and that it is easy to use a mass–radius relationship which accounts for the specific gravity and fall velocity changes caused by incorporation of water into aggregates. The primary disadvantage is that the number of particle size classes needed to describe a system increases faster than the square of the particle radius. Increasing i_{max} from 400 to 1600, a value 4 times as large, only increased the maximum particle radius from 144 to 257 μm, 1.84 times as large. Because the computational cost is on the order of i_{max}^2, this 84% increase in radius costs approximately 15 times more to compute. While using i to define the size classes is simple, it is too inefficient to use for computations over much larger size ranges.

Results show that increasing i_{max} from 400 to 1600 has little effect on smaller particles because they interact mostly with other small particles (Fig. 6). Most affected by an increase in size range are concentrations of larger particles and, as a result, the vertical flux

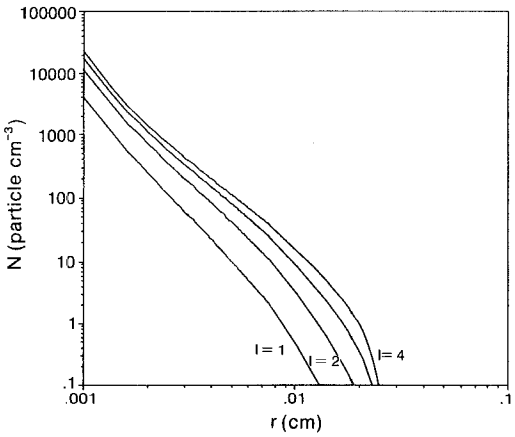

Fig. 9. Steady-state particle size spectra for four layers when the layers have, in order of increasing depth, γ = 0.4, 0.13, 0.08 and 0.057 s^{-1}. Other parameter values as in Fig. 8. $C_{1,1}$ and $C_{1,4}$ equal 2880 and 17,400 cell cm^{-3}. Slopes of lines fit through the log-transformed N as fn of r data for $r \leq 0.01$ cm were −3.64, −3.25, −2.97 and −2.84 for layers 1, 2, 3 and 4, respectively.

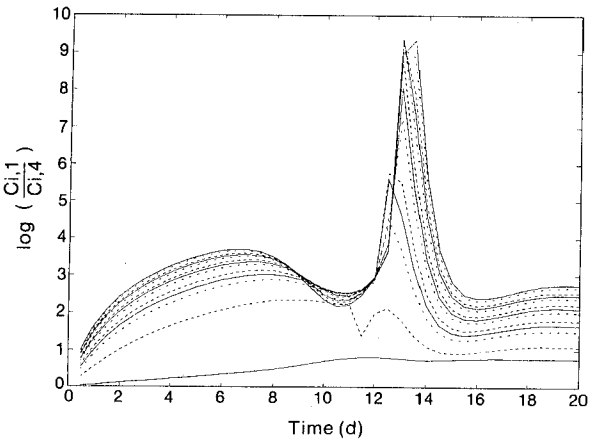

Fig. 10. Ratio of concentrations in layer 4 to those in layer 1 for $i = 1, 100, \ldots, 1600$ as functions of time. The large peak in ratios around day 14 is caused by the earlier coagulation regime in the deeper layer.

of matter (Fig. 4). As a result, this model underestimates the rate of vertical flux from the system.

Aggregate size in the environment does not increase indefinitely. Particles which become too large become vulnerable to break up by the same shear that brings particles together (SPIELMAN, 1978). A very crude estimate of the expected maximum particle diameter is the Kolmogorov length scale $(\nu/\gamma)^{0.5}$. For $\gamma = 2\ s^{-1}$ and $\nu = 0.01\ cm^2\ s^{-1}$, this is 0.07 cm, not that much larger than the diameter of the $i = 1600$ particle. Thus, incorporating particle breakup in the model is more important than indefinite increases in particles size classes.

Because real algae are seldom spheres, an important extension in this theory would be a more complete description of the role of shape. Species such as *Chaetoceros laciniosus* (RAYMONT, 1980) have spines which could enhance the effective size of the algal cell and thereby change interaction rates, as could formation of diatom chains. Information on how these affect interaction rates will best result from experimental observations.

C_{cr} and N_{cr} are overestimates of the actual equilibrium concentration because they do not account for algal removal by collision with aggregates. As a result, C_{cr} (1074 cell cm^{-3}) is almost 52% larger than the maximum value in the above simulations for single cell growth. However, such an error is small compared to the range of oceanic particle concentrations. The parameters C_{cr} and N_{cr} emphasize the interactions among such physiological variables as algal size, specific growth rate and stickiness, physical variables such as shear, and ecological variables such as algal concentration in determining the importance of coagulation. Given the large variations in the phytoplankton concentrations, specific growth rates, shears and α, C_{cr} and N_{cr} provide amazingly simple estimates of the coagulation potential of planktonic systems.

Efficiency of sticking after a collision is a function of chemical and hydrodynamic factors, including electrostatic repulsion of like-charged particles. Effects of electrostatic repulsion are much diminished in a high dielectric medium such as seawater, but other chemical factors, such as steric effects, could be important. Measurements of the coagulation of inorganic particles in seawater mixtures with salinity of 17.6‰ yielded α

values as high as 0.2 (GIBBS, 1983). Similar measurements on a mixture of living and dead particles in Swiss lakes yielded α values of 0.005–0.13 (WEILENMANN *et al.*, 1989). Organisms such as fungi grown in low ionic strength media are known to change their stickiness as a function of their metabolic states (ROSE, 1984). Such effects could occur with algae, manifesting themselves in changed values of C_{cr}. The common observation of aggregation in the high concentrations of algal cells in chemostats indicates that conditions are sometimes right for coagulations, implying that physiological state could be an important parameter in algal flocculation.

Shear rates in the ocean depend on a variety of factors, including depth and wind stress. The energy dissipation rate (ε) from wind stress has been related to $u_*^3 z^{-1}$, where z is the depth and u_* is the friction velocity (SOLOVIEV *et al.*, 1988). u_* is nearly proportional to the wind velocity above the surface boundary layer (GILL, 1982). The shear rate resulting from the energy dissipation can be estimated as $\gamma = (\varepsilon/(7.5\nu))^{0.5}$, where ν is the kinematic viscosity, about 10^{-2} cm^2 s^{-1} for seawater (MOUM and LUECK, 1985). A value for ε measured at 2 m during a modest wind of 6.0 m s^{-1} was about 0.04 cm^2 s^{-3}, equivalent to γ = 0.7 s^{-1} (SOLOVIEV *et al.*, 1988). Higher wind velocities will yield larger γ deeper. Assuming proportionality between u_* and wind speed, γ = 2 s^{-1} at 2 m when the wind speed is 12.1 m s^{-1}. Because of the importance of γ in determining C_{cr} and the short time needed to establish the coagulated state, a storm resulting in high γ could cause a situation where the algal concentration was previously lower than C_{cr} to become unstable, causing the formation of algal flocs and the increased sedimentation of organic matter. Furthermore, coagulation in the near-surface layer can trigger coagulation in deeper layers with lower shear.

Subdividing one well-mixed layer into otherwise identical well-mixed sublayers has several effects. The smaller mixed layer thicknesses (z vs z_l) increase the relative rates of loss due to settling (w_i/z_l). Because the large particles fall faster, there is a selective enrichment of larger particles in deeper layers. Lastly, because the flux leaving a layer when the system is at steady state equals the production in that layer plus the integrated production of the overlying layers, and because the flux is related to particle concentration, deeper layers have higher particle concentrations at steady state. Thus, stratification of a system changes the particle dynamics of a system, increasing the number of larger particles and speeding up the onset of coagulation but does not appreciably change the maximum concentration of solitary particles from that predicted using C_{cr}.

The decrease of shear with increasing depth and the increased flux of larger particles sedimenting from above will change the relative importance of the shear and differential sedimentation deeper in the water column. As a result, the particle size spectra and sedimentation rates should change with depth. Such changes have been observed in Bedford Basin (KRANCK and MILLIGAN, 1988) as well as in Swiss lakes (WEILENMANN *et al.*, 1989). The fact that the first step in coagulation of a bloom, the formation of the dimer, depends only on β_{S11} in the various shear layers emphasizes the utility of this simple coagulation model.

The algal bloom that emerges from consideration of model results starts with a rapidly growing population of single algal cells. During this phase, there is little loss of single cells to formation of aggregates or, therefore, to settling out of the euphotic zone. At a critical cell concentration, there is a rapid formation of aggregates. The critical cell concentration depends on cell sizes, cell surface properties, and environmental shear. The onset of the coagulation-dominated regime could be triggered by a combination of increase in the

turbulent shear from a passing storm, changing physiological state induced by nutrient depletion, slowing of algal growth, or settling of aggregates from an overlying layer. The coagulation process limits any further increases in algal concentrations despite continued cellular divisions. All production is funneled to large aggregates which, because of their sinking rates and large biomasses, move algal matter rapidly to the ocean benthos. Even if algae stop dividing, there will be continued loss of algal matter. The increase and any subsequent decrease of algal concentrations during an algal bloom need involve no intervention by animal grazing.

The effectively two-state nature of the algal system, in which coagulation is either not important or dominant, gives the results a simplicity that is expressed in C_{cr} and N_{cr}. It is, therefore, easy to see that the critical concentrations would be twice as large as those shown (Fig. 7) if the shear were 1 s^{-1} rather than the 2 s^{-1} previously used (Fig. 2), or half as large if α were 0.5 rather than the 0.25 also previously used.

Furthermore, the rapid transition between the two states gives the results a generality beyond that of a situation where all parameters are constant. If algal cells deplete the dissolved nutrients, change their nutritional status and increase their stickiness, the coagulation tendency of the new system can be estimated by comparing particle concentrations with the new C_{cr}. If the particle concentrations are greater than C_{cr}, there will be a rapid loss of particles to coagulation and a decrease in particle concentration. Similarly, if a storm event increases turbulent shear, its potential for triggering rapid coagulation can be assessed in the same way. While this approach by itself does not predict changes in coagulation rate or particle size spectrum, it does allow one to assess the coagulation potential of a given situation and to predict the expected changes.

That coagulation of phytoplankton blooms can occur in natural systems is known from observations in lakes (WEILENMANN *et al.*, 1989) as well as a coastal basin (KRANCK and MILLIGAN, 1988). This model explores the consequences of such coagulation and, in C_{cr} provides a simple way to estimate the coagulation potential of a system. Formation of algal aggregates, observed both in laboratory algal blooms (RIEBESELL, 1989) as well as in the field (e.g. SMETACEK, 1985; ALLDREDGE and GOTSCHALK, 1988a) are the result of high algal concentrations and, possibly, physiological changes which affect algal stickiness. The fact that the observed aggregates tend to be composed of large diatoms rather than smaller species, such as coccolithophores (ALLDREDGE and GOTSCHALK, 1988a; ALLDREDGE and SILVER, 1988), is consistent with the higher encounter rates associated with the larger particles.

The presence of algal mats on the ocean floor soon after surface algal blooms (BILLET *et al.*, 1983; LOCHTE and TURLEY, 1988) is a consequence of the formation of large, rapidly sinking aggregates which need not be produced or transformed by herbivores or algae. Such rapid movement of algal movement could account for the carbon transport from the euphotic zone that WALSH (1983) has postulated to balance carbon budgets.

Bacteria and cyanobacteria have been reported in algal flocs found on the bottom of the North Atlantic at 4500 m (LOCHTE and TURLEY, 1988). Because cyanobacterial biomass was less than 1% of total floc biomass, it is unclear from the report whether the dominant biological source of the floc was a larger algal species or the smaller bacteria and cyanobacteria. Concentrations of cyanobacteria in the surface waters at the time were 5×10^5 cells cm^{-3}, about 6% of the C_{cr} calculated for $r_1 = 0.5\ \mu m$ above. Such smaller cells were probably not the main component of algal coagulation but could have been entrained by coagulation of large cells.

Recent descriptions of planktonic systems have tended to emphasize easily measured composite system parameters such as particle organic carbon and chlorophyll pigment concentrations. Such parameters do not provide enough information to assess the coagulation potential of a system. EVANS (1988) concluded from phytoplankton models that phytoplankton should be perceived as more than just chlorophyll concentrations. The model presented here emphasizes this for field observations as well as models. Useful descriptions of phytoplankton populations include the particle size distributions made popular by SHELDON *et al.* (1972), as well as observations on the stickiness of the particles. With measurements of size and algal abundance the parameters C_{cr} and N_{cr} can be estimated and compared with natural particle concentrations to assess the conditions for floc formation.

Particle size spectra in the ocean show characteristic patterns that can provide insight into particle dynamics. The slope of the line relating log N to log r is typically around -3 in oceanic environments (e.g. MCCAVE, 1984). The slope for the models where all divisions were from solitary cells ranged from -3.6 to -2.6, with the less negative results resulting in waters which were being influenced by coagulation in overlying waters (Figs 8 and 9). Slopes are even less negative when there is also division in aggregates, -2.4 in the case calculated here (Fig. 3). LOGAN and ALLDREDGE (1989) have argued that nutrient supply to algae in aggregates is enchanced by fluid flow, implying that nutrient limitation in aggregates need not limit algal growth to solitary cells. The differences between the results for the two different aggregation models suggest that the two growth mechanisms may be distinguished in the field by the slopes of their size spectra.

This model has emphasized the balance between algal growth and coagulation, showing that coagulation dominates when single cell concentrations reach a critical concentration. Coagulation processes occur at particle concentrations lower than these, although not at such a rapid rate, and effectively place an upper bound on particle abundances. It may be significant that the highest reported algal concentrations in such high productivity regions as the Antarctic Ocean, North Pacific, and coastal waters off New York are close to 1000 cell cm^{-3}, very similar to the C_{cr} developed under the simulation conditions (MARUMO, 1967; KOZLOVA, 1970; ZERNOVA, 1970; HULBURT, 1970). In the more complicated situation, where zooplankton and bacterial communities consume substantial parts of algal production, coagulation may not be as rapid. However, a non-biologically selective mechanism for removal of particles could have an important role in removing some of the odd particles.

Algal blooms are situations inherently out of balance, where algal growth exceeds the ability of biological processes to control it. Physical coagulation processes place an upper bound on the accumulation of such blooms. In the process, they can lead to rapid formation of the algal flocs commonly observed by divers. Coagulation forms an additional dimension for the behavior of marine planktonic systems.

Acknowledgements—I am grateful for conversations held with Jim Morgan, Charlie O'Melia and Thomas Kiørboe. This work was supported by Office of Naval Research contract N00014 87-K0005 and U.S. Department of Energy grant DE-FG05-85-ER60341.

REFERENCES

ALLDREDGE A. L. and C. C. GOTSCHALK (1988a) Direct observations of the mass flocculation of diatom blooms: characteristics, settling velocities and formation of diatom aggregates. *Deep-Sea Research*, **36**, 159–171.

ALLDREDGE A. L. and C. GOTSCHALK (1988b) *In situ* settling behavior of marine snow. *Limnology and Oceanography*, **33**, 339–351.

ALLDREDGE A. L. and M. W. SILVER (1988) Characteristics, dynamics and significance of marine snow. *Progress in Oceanography*, **20**, 41–82.

BILLET D. S. M., R. S. LAMPITT, A. L. RICE and R. F. C. MANTOURA (1983) Seasonal sedimentation of phytoplankton to the deep-sea benthos. *Nature*, **302**, 520–522.

EVANS G. T. (1988) A framework for discussing seasonal succession and coexistence of phytoplankton species. *Limnology and Oceanography*, **33**, 1027–1036.

GIBBS R. J. (1983) Effect of organic coatings on the coagulation of particles. *Environmental Science and Technology*, **17**, 237–240.

GILL A. E. (1982) *Atmosphere–ocean dynamics*. Academic Press, San Diego, 662 pp.

HULBURT E. M. (1970) Competition for nutrients by marine phytoplankton in oceanic, coastal, and estuarine regions. *Ecology*, **51**, 475–484.

HUNT J. R. (1982) Particle dynamics in seawater: implication for predicting the fate of discharged particles. *Environmental Science and Technology*, **16**, 303–309.

JACKSON G. A. (1989) Simulation of bacterial attraction and adhesion to falling particles in an aquatic environment. *Limnology and Oceanography*, **34**, 514–530.

KOZLOVA O. G. (1970) Diatoms in suspension and in bottom sediments in the southern Indian and Pacific Oceans. In: *Antarctic ecology*, Vol. 1, M. W. HOLDGATE, editor, Academic Press, New York, pp. 136–142.

KRANCK K. and T. MILLIGAN (1980) Macroflocs: production of marine snow in the laboratory. *Marine Ecology Progress Series*, **3**, 19–24.

KRANCK K. and T. MILLIGAN (1988) Macroflocs from diatoms: *in situ* photography of particles in Bedford Basin, Nova Scotia. *Marine Ecology Progress Series*, **4**, 183–189.

LOCHTE K. and C. M. TURLEY (1988) Bacteria and cyanobacteria associated with phytodetritus in the deep sea. *Nature*, **333**, 67–69.

LOGAN B. E. and A. L. ALLDREDGE (1989) The increased potential for nutrient uptake by flocculating diatoms. *Marine Biology*, **101**, 443–450.

MARUMO R. (1967) General features of diatom communities in the North Pacific Ocean in summer. *Information Bulletin of Planktology in Japan*, **12**, 115–121.

MCCAVE I. N. (1984) Size spectra and aggregation of suspended particles in the deep ocean. *Deep-Sea Research*, **31**, 329–352.

MOUM J. N. and R. G. LUECK (1985) Causes and implications of noise in oceanic dissipation measurements. *Deep-Sea Research*, **32**, 379–392.

MULLIN M. M., P. R. SLOAN and R. W. EPPLEY (1966) Relationship between carbon content, cell volume, and area in phytoplankton. *Limnology and Oceanography*, **11**, 307–311.

O'MELIA C. R. (1972) An approach to modeling of lakes. *Schweizer Zeitschrift fur Hydrologie*, **34**, 1–33.

O'MELIA C. R. and K. S. BOWMAN (1984) Origins and effects of coagulation in lakes. *Schweizer Zeitschrift fur Hydrologie*, **46**, 64–85.

PARSONS T. R., K. STEPHENS and J. D. H. STRICKLAND (1961) On the chemical composition of eleven species of marine phytoplankters. *Journal of the Fisheries Research Board of Canada*, **18**, 1001–1016.

PRUPPACHER H. R. and J. D. KLETT (1980) *Microphysics of clouds and precipitation*. Riedel, Boston, 714 pp.

RAYMONT J. E. G. (1980) *Plankton and productivity in the oceans*, 2nd edn, Vol. 1, Pergamon, Oxford, 489 pp.

RIEBESELL U. (1989) Comparison of sinking and sedimentation rate measurements in a diatom winter/spring bloom. *Marine Ecology Progress Series*, **54**, 109–119.

ROSE A. H. (1984) Physiology of cell aggregation: flocculation by *Saccharomyces cerevisiae* as a model system. In: *Microbial adhesion and aggregation*, K. C. MARSHAL, editor, Springer Verlag, New York, pp. 323–335.

SHANKS A. L. and E. W. EDMONDSON (1989) Laboratory-made artificial marine snow—a biological model of the real thing. *Marine Biology*, **101**, 463–470.

SHELDON R. W., A. PRAKASH and W. H. SUTCLIFFE (1972) The size distribution of particles in the ocean. *Limnology and Oceanography*, **17**, 327–340.

SMAYDA T. R. (1970) The suspension and sinking of phytoplankton in the sea. *Oceanography and Marine Biology, Annual Review*, **8**, 353–414.

SMETACEK V. S. (1985) Role of sinking in diatom life-history cycles: ecological, evolutionary and geological significance. *Marine Biology*, **84**, 239–251.

SMETACEK V. and F. POLLEHNE (1986) Nutrient cycling in pelagic systems: a reappraisal of the conceptual framework. *Ophelia*, **26**, 401–428.

Soloviev A. V., N. V. Vershinsky and V. A. Bezverchnii (1988) Small-scale turbulence measurements in the thin surface layer of the ocean. *Deep-Sea Research*, **35**, 1859–1874.

Spielman L. A. (1978) Hydrodynamic aspects of flocculation. In: *The scientific basis of flocculation*, K. J. Ives, editor, Sijthoff and Noordhoff, Alphen aan den Rijn, The Netherlands, pp. 63–88.

Walsh J. J. (1983) Death in the sea: enigmatic phytoplankton losses. *Progress in Oceanography*, **12**, 1–86.

Weilenmann U., C. R. O'Melia and W. Stumm (1989) Particle transport in lakes: models and measurements. *Limnology and Oceanography*, **34**, 1–18.

Zernova V. V. (1970) Phytoplankton of the Southern Ocean. In: *Antarctic ecology*, Vol. 1, M. W. Holdgate, editor, Academic Press, New York, pp. 148–153.